

Two new catalogs of blazar candidates in the *WISE* infrared sky

RAFFAELE D'ABRUSCO,¹ NURIA ÁLVAREZ CRESPO,^{2,3} FRANCESCO MASSARO,^{2,4,5} RICCARDO CAMPANA,⁶
VAHRAM CHAVUSHYAN,⁷ MARCO LANDONI,⁸ FABIO LA FRANCA,⁹ NICOLA MASETTI,^{6,10} DAN MILISAVLJEVIC,¹¹
ALESSANDRO PAGGI,^{2,4,5} FEDERICA RICCI,¹² AND HOWARD A. SMITH¹

¹*Center for Astrophysics | Harvard & Smithsonian, 60 Garden Street, Cambridge, MA 20138, USA*

²*Dipartimento di Fisica, Università degli Studi di Torino, via Pietro Giuria 1, I-10125 Torino, Italy*

³*European Space Agency (ESA), European Space Astronomy Centre (ESAC), E-28691 Villanueva de la Cañada, Madrid, Spain*

⁴*Istituto Nazionale di Fisica Nucleare, Sezione di Torino, via Pietro Giuria 1, I-10125 Torino, Italy*

⁵*INAF - Osservatorio Astrofisico di Torino, via Osservatorio 20, I-10025 Pino Torinese, Italy*

⁶*INAF - Osservatorio di Astrofisica e Scienza dello Spazio, via Gobetti 93/3, I-40129, Bologna, Italy*

⁷*Instituto Nacional de Astrofísica, Óptica y Electrónica, Apartado Postal 51 y 216, 72000 Puebla, México*

⁸*INAF - Istituto Nazionale di Astrofisica, via Emilio Bianchi 46, I-23807 Merate (LC), Italy*

⁹*Dipartimento di Matematica e Fisica, Università Roma Tre, via della Vasca Navale 84, I-00146, Roma, Italy*

¹⁰*Departamento de Ciencias Físicas, Universidad Andrés Bello, Fernández Concha 700, Las Condes, Santiago, Chile*

¹¹*Department of Physics and Astronomy, Purdue University, 525 Northwestern Avenue, West Lafayette, IN, 47907, USA*

¹²*Instituto de Astrofísica and Centro de Astroingeniería, Facultad de Física, Pontificia Universidad Católica de Chile, Casilla 306, Santiago 22, Chile*

(Received; Revised; Accepted)

ABSTRACT

We present two catalogs of radio-loud candidate blazars whose *WISE* mid-infrared colors are selected to be consistent with the colors of confirmed γ -ray emitting blazars. The first catalog is the improved and expanded release of the WIBRaLS catalog presented by D'Abrusco et al. (2014): it includes sources detected in all four *WISE* filters, spatially cross-matched with radio source in one of three radio surveys and radio-loud based on their q_{22} spectral parameter. WIBRaLS2 includes 9541 sources classified as BL Lacs, FSRQs or mixed candidates based on their *WISE* colors. The second catalog, called KDEBLLACS, based on a new selection technique, contains 5579 candidate BL Lacs extracted from the population of *WISE* sources detected in the first three *WISE* passbands ([3.4], [4.6] and [12]) only, whose mid-infrared colors are similar to those of confirmed, γ -ray BL Lacs. KDEBLLACS members area also required to have a radio counterpart and be radio-loud based on the parameter q_{12} , defined similarly to q_{22} used for the WIBRaLS2. We describe the properties of these catalogs and compare them with the largest samples of confirmed and candidate blazars in the literature. We crossmatch the two new catalogs with the most recent catalogs of γ -ray sources detected by *Fermi* LAT instrument. Since spectroscopic observations of candidate blazars from the first WIBRaLS catalog within the uncertainty regions of γ -ray unassociated sources confirmed that $\sim 90\%$ of these candidates are blazars, we anticipate that these new catalogs will play again an important role in the identification of the γ -ray sky.

Keywords: BL Lacertae objects: general - catalogs - galaxies: active - radiation mechanisms: non-thermal

1. INTRODUCTION

Blazars represent one of the most extreme classes of active galactic nuclei (AGNs). These radio-loud sources are characterized by flat radio spectra even at low radio frequencies (i.e., below ~ 1 GHz) (Massaro et al. 2013a,b; Nori et

al. 2014; Giroletti et al. 2016), superluminal motions (see e.g., Vermeulen, & Cohen 1994; Lister, & Homan 2005; Lister et al. 2009, and references therein), peculiar infrared colors (Massaro et al. 2011; D'Abrusco et al. 2014, hereinafter Paper I), high optical polarization (see e.g., Agudo et al. 2014; Pavlidou et al. 2014; Angelakis et al. 2016; Hovatta et al. 2016) and, not least, rapid and irregular variability (see e.g., Homan et al. 2002) at all frequencies with uncorrelated amplitudes and different time scales ranging between minutes to weeks (Homan et al. 2002). Blazars can reach bolometric luminosities up to 10^{49} erg s $^{-1}$ during γ -ray flaring states (Oriente et al. 2014).

The emission from blazars, according to the unification scenario of radio-loud AGNs, arises from a relativistic jet, closely aligned along the line of sight, that, in some cases, can outshine the host galaxy and the other AGN emission components (see e.g., Blandford, & Rees 1978; Urry, & Padovani 1995).

A close connection between the γ -ray and the infrared (IR) properties of blazars has recently emerged from the investigation of the all-sky surveys carried out with Wide-Field Infrared Survey Explorer (*WISE*) (Wright et al. 2010) and *Fermi* satellites (D'Abrusco et al. 2012; Massaro et al. 2016). The observed correlations across more than 10 decades of frequency has been proven to be an extremely powerful tool to identify new γ -ray emitting blazars among *Fermi* sources with unknown or uncertain lower-energy counterparts (Massaro et al. 2012a; D'Abrusco et al. 2013).

With a sky density of ~ 0.1 sources per square degree, blazars dominate the γ -ray sky in the MeV-TeV energy range and represent $\sim 40\%$ of the sources in the Third *Fermi*-Large Area Telescope (LAT) Source Catalog (3FGL, Acero et al. 2015; Massaro et al. 2015). Blazars are mainly divided into two sub-classes based on their optical spectra: (i) BL Lac objects characterized by featureless optical spectra or showing emission and/or absorption lines of equivalent widths $EW < 5\text{\AA}$ (Stickel et al. 1991; Falomo et al. 2014), and (ii) Flat Spectrum Radio Quasars (FSRQs) with a typical quasar-like optical spectrum. Hereinafter, we adopt the nomenclature used in the Roma-BZCAT catalog (Massaro et al. 2009, 2015), where BL Lacs and FSRQs are referred to as BZBs and BZQs, respectively.

The Spectral Energy Distributions (SEDs) of blazars are characterized by two broad components, a low-energy one peaking between the IR and X-ray bands and a high energy one whose emission ranges between the X-rays and the γ -rays. The former component is interpreted as synchrotron radiation from relativistic particles accelerated in a jet while the component at higher energies, according to leptonic models, is due to inverse Compton emission with seed photons that can have different origins (for more details see e.g., Böttcher 2007, 2012), while hadronic models invoke the synchrotron emission by protons or secondary particles produced in proton-photon interactions (Dermer, & Schlickeiser 1993; Mücke, & Protheroe 2001; Murase et al. 2012, and references therein).

The BL Lac population is also divided, according to their SEDs, in “Low-frequency peaked BL Lac objects” (LBLs) when the peak of the first component lie in the IR-to-optical energy range and “High-frequency peaked BL Lac objects” (HBLs) when the synchrotron peak falls in the UV-to-X-rays energy range (Padovani, & Giommi 1996). Another, more recent classification distinguishes blazars as low-synchrotron peaked (LSP), intermediate-synchrotron peaked (ISP) or high-synchrotron peaked (HSP) based on the peak frequency $\nu_{S,\text{peak}}$ of the synchrotron component of their SEDs (Abdo et al. 2010; Ackermann et al. 2015). Here we will adopt the LBLs/HBLs sub-classification for the BZBs as it does not strictly depend on the exact location of the peak frequency.

The discovery of the peculiar *WISE* IR colors of blazars has been used to search for blazar-like sources within the positional uncertainty regions of the unidentified/unassociated γ -ray sources (UGSs) that could be their potential counterparts (see e.g., Massaro et al. 2015). Several procedures based on *WISE* data have been developed to investigate the nature of the UGSs listed in all *Fermi* source catalogs as well as to verify the nature of blazars candidates of uncertain type (BCUs; Massaro et al. 2012b; Cowperthwaite et al. 2013; Álvarez Crespo et al. 2016a). However, all these methods require spectroscopic confirmation of the natures of the blazar candidates selected.

One of the largest sources of candidate blazars used to identify unassociated γ -ray sources observed by the *Fermi* LAT has been the catalog of *WISE* Blazar-Like Radio-Loud Sources (WIBRaLS; Paper I). This catalog contains *WISE* sources detected in all four *WISE* bands, whose mid-IR colors are similar to those of confirmed *Fermi* blazars. WIBRaLS sources were also required to a) have a radio counterpart from one of three major surveys, namely the National Radio Astronomy Observatories Very Large Array VLA Sky Survey (NVSS, Condon et al. 1998) the VLA Faint Images of the Radio Sky at Twenty-cm Survey (FIRST, White et al. 1997; Helfand et al. 2015) and the Sydney University Molonglo Sky Survey Source Catalog (SUMSS, Mauch et al. 2003), and b) to be radio-loud, that is to have an observed ratio between radio and $22\text{ }\mu\text{m}$ mid-infrared flux densities > 3 (Paper I).

Since the publication of the WIBRaLS catalog, extensive optical spectroscopic campaigns whose goal is to verify the nature of WIBRaLS1 blazar candidates that can be spatially associated to γ -ray sources observed by *Fermi* have been carried out (see e.g., Massaro et al. 2014; Paggi et al. 2014; La Mura et al. 2015; Landoni et al. 2015; Massaro

et al. 2015; Ricci et al. 2015; Ajello et al. 2017a; Álvarez Crespo et al. 2016a,b,c; Peña-Herazo et al. 2017; Paiano et al. 2017a,b; Landoni et al. 2018; Marchesi et al. 2018; Paiano et al. 2019; Marchesini et al. 2019). The total number of WIBRaLS candidate blazars which have been spectroscopically followed up and reported upon in either one of the papers listed above is, to date, 159 split in 126 candidate BZBs, 16 candidate BZQs and 17 candidates with no spectral classification available (Mixed). The analysis of the optical spectra confirmed that $\sim 93\%$ of candidate BZBs have featureless optical spectra typical of BL Lacs and $\sim 52\%$ of the candidate BZQs show FSRQ spectra. Only $\sim 3\%$, $\sim 12\%$ and $\sim 11\%$ of the spectra of observed candidate BZBs, BZQs or Mixed blazars cannot be classified as belonging to blazars, yielding a weighted average efficiency of the selection $\sim 95\%$. Checks of spectra already published in the literature for 28 additional candidate blazars from WIBRaLS1 confirmed a BL Lacs or FSRQs nature for 27 of them.

Since the publication of the first release of the WIBRaLS catalog (Paper I), new versions of some of the main datasets used to define its selection method have been released:

- The ROMA BZCat, which contains the list of *bona fide*, spectroscopically confirmed blazars used to define the *locus* occupied by γ -ray emitting blazars in the *WISE* color space, has reached its 5th release (Massaro et al. 2009). This release contains ~ 3600 sources, vs ~ 3050 sources in the version used by D’Abrusco et al. (2014).
- The LAT 3-year Point Source Catalog (3FGL) (Acero et al. 2015) of γ -ray sources detected by *Fermi* containing ~ 3000 sources, has also become available. This recent update to the catalog of *Fermi* LAT sources is more than twice as large as the 2-year 2FGL (Nolan et al. 2012) catalog (~ 2250 members) used to extract the first version of the WIBRaLS catalog.

These two new datasets yield jointly a larger sample of confirmed γ -ray blazars that can be used to characterize more accurately their *WISE* mid-IR properties and hence to identify more effectively blazars that may be detected in the γ -ray energy range. In this paper we describe a new release of the WIBRaLS catalog that, by taking advantage of these most recent data available, maximizes the legacy value of *WISE* observations for the investigation of blazars.

The completeness of the WIBRaLS catalog is a function of the blazar spectral class, and decreases significantly for BL Lacs, which often are not detected in the $[22] \mu\text{m}$ *WISE* band. BZBs, in particular HBLs, have lower detection rate in the $[22] \mu\text{m}$ *WISE* band (Paper I), since their emission in the mid-infrared at $22 \mu\text{m}$ may be lower than the limiting sensitivity in the fourth *WISE* band.

For this reason, in this paper we will also present a new, complementary catalog of candidate BZBs selected with a novel technique that employs the *WISE* colors obtained from the first three *WISE* bands only and has been applied to All*WISE* sources not detected in W4. We focus only on the BZB spectral class for two main reasons: i) the region of the IR color-color space occupied by BZB is less contaminated by spurious IR sources than that of BZQs, ii) during our campaign of spectroscopic follow-up of candidate BL Lacs selected with *WISE* colors, we found that a large fraction of UGSs and BCUs are classified as candidate BZBs, providing an indication that they are the most elusive counterparts of *Fermi* sources (70.5 % and 65.4 %, respectively, see Massaro, & D’Abrusco 2016).

The paper is organized as follows: in Section 2 we provide a brief introduction to the *WISE* and radio catalogs used to extract both samples of candidate blazars. Sections 3 and 4 describe the selection methods of the new WIBRaLS catalog and the catalog of BL Lac candidates selected using two *WISE* colors only, respectively. The comparison between the two catalogs presented in this paper and the literature is described in Section 5. Finally, our conclusions are summarized in Section 6.

We use cgs units unless otherwise stated and spectral indices, α , are defined by flux density $S_\nu \propto \nu^{-\alpha}$ indicating as flat spectra those with $\alpha < 0.5$. *WISE* magnitudes used here are in the Vega system and are not corrected for the Galactic extinction. As shown in our previous analyses (D’Abrusco et al. 2013, 2014), such correction affects only the magnitude at $3.4 \mu\text{m}$ for sources lying at low Galactic latitudes, and it ranges between 2% and 5% of the magnitude, thus not affecting significantly our results.

2. DATA

2.1. Infrared data

All the candidate blazars discussed in this paper were sources extracted from images produced by the *WISE* space telescope (Wright et al. 2010). *WISE* has observed the whole sky from 2009 to 2011 in the four bands W1, W2, W3 and W4 centered on 3.4 , 4.6 , 12 and $22 \mu\text{m}$, respectively.

The All*WISE* source catalog has superseded the previously available *WISE* All-Sky catalog; it was produced by combining *WISE* single exposures images from the first two years of the mission with the post-cryogenic phase data (Mainzer

et al. 2011), that observed the sky in three (W1, W2 and W3) and then only two (W1 and W2) bands. The final result is a two-fold improvement in the depth-of-coverage in the first two bands thanks to the additional observations that have increased the sensitivity of the stacked images, and improved photometric accuracy in all filters thanks to updated background measurements. The All *WISE* sensitivities are 54, 71, 730 and 5000 μ Jy in the W1, W2, W3 and W4 passbands respectively, with angular resolutions of 6".1, 6".4, 6".5 and 12". Due to the *WISE* survey strategy, the limiting sensitivity of the catalog of sources extracted from the *WISE* images is not uniform on the sky (compare with Figure 8 at the Explanatory Supplement to the All *WISE* Data Release Products¹).

The All *WISE* Source Catalog contains astrometry and photometry in the IR for 747,634,026 objects; only 25,882,082 of these sources ($\sim 3.5\%$) were seen in all the four bands, increasing up to 99,118,890 sources ($\sim 13.3\%$) detected in the first three bands W1, W2 and W3 only. These two catalogs represent the parent samples for the updated WIBRaLS (Section 3) and the new catalog of BL Lacs candidates (Section 4), respectively.

2.2. Radio data

We have crossmatched the catalog of All *WISE* sources according to the procedure described in Section 3.2 with the NVSS, the FIRST and the SUMSS radio surveys. A brief description for each of these three radio surveys is given below.

- NVSS (Condon et al. 1998) is a 1.4 GHz continuum survey performed using the Very Large Array (VLA) and covering the entire sky north of -40 deg declination, i.e. 82% of the celestial sphere with a beam size of 45" FWHM. The result is a catalog of over 1.8 million discrete sources brighter than $S \sim 2.5$ mJy in the entire survey.
- FIRST (White et al. 1997; Helfand et al. 2015) is a project designed to produce the radio equivalent of the Palomar Observatory Sky Survey over 10,000 square degrees of the North and South Galactic Caps using the NRAO Very Large Array (VLA). The beam size varies between 5".4 FWHM for circular beam and 6".8 along the major axis for elliptical shape, as a function of the declination of the observation. The survey area has been chosen to coincide with that of the Sloan Digital Sky Survey (SDSS, see e.g., Gunn et al. 1998) and at the $m_v \sim 23$ limit of SDSS, $\sim 40\%$ of the optical counterparts to FIRST sources are detected. At the 1 mJy source detection threshold, there are ~ 90 sources per square degree.
- SUMSS (Mauch et al. 2003) is a radio imaging survey of the southern sky carried out with the Molonglo Observatory Synthesis Telescope (MOST) operating at 843 MHz, with a beam size $\approx 43''$ FWHM. The catalog covers approximately 3500 deg² with declination $\delta < -30^\circ$, about 43% of the total survey area. The survey has a limiting peak brightness of 6 mJy/beam at declinations $\delta \leq -50^\circ$, and 10 mJy/beam at $\delta > -50^\circ$. The SUMSS is therefore similar in sensitivity and resolution to the NVSS, with ~ 7000 sources found in the overlap region.

3. THE SECOND RELEASE OF THE WIBRALS CATALOG

In this paper, a new release of the catalog of *WISE* Blazar-like RAdio-Loud Sources (WIBRaLS) has been built up by following an improved version of the procedure described by Paper I and including new samples of confirmed blazars associated with *Fermi* γ -ray sources. Schematically, the steps we followed to extract the WIBRaLS catalog are the following:

1. We select *WISE* sources detected in all four *WISE* bands, with IR colors similar to those of associated *Fermi* blazars (Section 3.1). We call these sources "*WISE* blazar-like sources".
2. The *WISE* blazar-like sources are positionally cross-matched with sources extracted from either one of the radio surveys NVSS, SUMSS and FIRST (Section 3.2) and only those with a radio counterpart are retained.
3. Among the *WISE* blazar-like sources with a radio counterpart, only radio-loud sources are selected as members of the WIBRaLS catalog (Section 3.3).

In the following, we provide descriptions of each step above.

¹ <http://wise2.ipac.caltech.edu/docs/release/allwise/expsup/sec4.2.html>

3.1. *WISE* color selection of blazar-like sources

We define the blazar-like *locus* using the sample of confirmed *Fermi* blazars, based on the 5th version of the ROMA-BZCat catalog (Massaro et al. 2015) and the 3FGL catalog (Acero et al. 2015), associated with All *WISE* counterparts detected in all four *WISE* filters. This *locus* thus includes newly identified 4-band sources and extends the *locus* presented in Paper I.

The BZCat v.5.0 contains 3561 *bona fide* blazars with spectroscopic confirmation. Optical spectra are also used to classify members of the BZCat as BZBs or BZQs, according to the total equivalent width of all emission and absorption features, while blazars whose properties are intermediate between BZB and BZQ are tagged as Uncertain (BZU) and other blazar-like objects whose emission is mostly contaminated by light from the host galaxy are labeled as BZGs.

All BZCat sources classified as BZU and BZG were discarded, leaving 1151 BZBs and 1909 BZQs. In order to spatially crossmatch the positions of these BZCat sources with All *WISE* sources detected in the four filters, we adopted the maximum radial distance of 3''.3 obtained by conservatively combining a nominal uncertainty of 1'' on the radio positions of BZCat sources with positional uncertainty in the *WISE* W4 passband (see D'Abrusco et al. 2013, for details). This sample was then spatially crossmatched with γ -ray sources included in the 3FGL catalog (Acero et al. 2015), the latest release of sources detected by the LAT instrument on board NASA's *Fermi* spacecraft, based on the first 48 months of survey data. The crossmatch has been performed by taking into account the position angles and the lengths of the semi-major and semi-minor axes of the 95% confidence region of each *Fermi* source, available in 3FGL, and the positional uncertainty of the All *WISE* counterparts of the BZCat sources. The final sample used to define the *WISE* three-dimensional *locus* consists of 901 confirmed γ -ray emitting blazars, split in 497 BZBs and 404 BZQs, and is more than twice as large as the analogous list in Paper I, which contained 447 sources.

Following Paper I, we define a model of the *locus* in the three-dimensional Principal Components (PCs) space generated by the three independent *WISE* colors W1-W2 ([3.4]-[4.6]), W2-W3 ([4.6]-[12]) and W3-W4 ([12]-[22]). The *locus* is modeled as a set of three coaxial cylinders whose axes lie on the direction of the first PC (PC1). The two extremal cylinders are populated by blazars of similar spectral classes, namely BZB and BZQ respectively, while the intermediate cylinder contains significant ($\geq 25\%$) fractions of both BZBs and BZQs. The length along the PC1 axis of the two extremal cylinders is defined so that they contain at least 75% of blazars classified as candidate BZBs and BZQs, respectively, while excluding the *locus* sources with PC1 value smaller than the 1%-st percentile and larger than the 99%-th percentile of the distribution of *locus* PC1 coordinates. The mixed cylinder contains fractions of BZBs and BZQs each smaller than 75%. The radii of the three cylinders, which lie in the plane generated by PC2 and PC3 and orthogonal to PC1, are defined to contain 95% of the sources whose PC1 coordinates fall in each of the three cylinders. Sources located within the *locus* are selected on the base of the value of their "score", a quantitative measure of the distance of a generic source to the *locus* model, defined as follows.

The *WISE* colors of a *WISE* source and the associated uncertainties are projected into the PC three-dimensional space, where they define an "uncertainty ellipsoid". The position and orientation of this ellipsoid - relative to the model of each cylinder separately - are used to calculate a numeric value defined between 0 and 1. This normalized distance is then weighted by the volume of the error ellipsoid, so that two *WISE* sources placed in the same position relative to the *locus* model but with different uncertainties are assigned different scores. A more detailed description of the score and its properties can be found in Paper I.

The score is also used to classify candidate blazars compatible with the model of the *locus* according to their reliability. All *WISE* sources with non-zero score for either cylinder are ranked according to the decreasing compatibility with the *locus* model in the classes A, B, C and D, defined by the 90%-th, 60%-th, 20%-th and 5%-th percentiles of the *score* distribution for the sources of the *locus* sample. These classes are defined to facilitate quick prioritization of candidate blazars as targets of follow-up observation across sources of different spectral types (BZB-like, BZQ-like or Mixed) and regardless of the specific *score* distributions for each spectral type. Nonetheless, classes do not replace *scores* as a quantitative indicator of the degree of compatibility of each candidate blazar with the *locus* model in the *WISE* color space; all scientific analysis on the final list of WIBRaLS should be performed using *scores*. The lower 5% threshold corresponds to the fraction of *locus* sources that are located outside the *locus* model by definition. The values of the *score* thresholds used to define the three classes are reported in Table 3.1.

To all sources with score larger than the 5-th percentile threshold, for any one of the three cylinders, are assigned the corresponding type (BZB, BZQ or Mixed) and selected as *WISE* blazar-like sources. The Mixed type does indicate a specific spectral class, since the Mixed cylinder contains comparable fractions of both BZBs and BZQs.

. These values are determined as the 5%-th, 20%-th, 60%-th and 90%-th percentiles of the distribution of *scores* of the *locus* sample, separately for BZB, Mixed and BZQ cylinders in the *locus* model.

Table 1. Values of the *score* thresholds $s_{5\%}$, $s_{20\%}$, $s_{60\%}$ and $s_{90\%}$, used for the extraction of the *WISE* blazar-like sources and to define the classes as described in Section 3.1

	BZB-like	Mixed	BZQ-like
$s_{5\%}$ (D)	0.24	0.32	0.22
$s_{20\%}$ (C)	0.51	0.54	0.48
$s_{60\%}$ (B)	0.74	0.85	0.77
$s_{90\%}$ (A)	0.91	0.99	0.91

The total number of *WISE* blazar-like sources selected is 526,681, split in 156,506 BZB candidates ($\sim 30\%$), 348,805 ($\sim 60\%$) BZQ candidates and the remaining 21,370 ($\sim 4\%$) sources located in the Mixed region. The *WISE* blazar-like sources can also be split in 7,807 Class A sources ($\sim 1\%$), 27,986 Class B sources ($\sim 5\%$), 149,052 Class C sources ($\sim 28\%$) and the remaining 341,836 ($\sim 65\%$) belonging to the class D.

3.2. Radio counterparts

Following Paper I, we determined the optimal radii for the association of the *WISE* blazar-like sources with their potential radio counterpart in the NVSS, SUMSS and FIRST surveys.

We adopted a modified version of the procedure illustrated by Best et al. (2005) and Donoso et al. (2009). They computed the optimal radius for the spatial crossmatch of NVSS and FIRST radio detections with optical sources in SDSS by setting a threshold on the fraction of spurious associations (i.e. the contamination) obtained for different values of maximum crossmatch radius. In this paper, similarly at what done in Paper I, the optimal association radius is indeed set as the radial distance that provides a given fixed efficiency of the selection $e_{\text{thr}} = 99\%$, corresponding to a contamination $c_{\text{thr}} = 1\%$, where $c(\vartheta) = 100\% - e(\vartheta)$. The efficiency or purity of the selection is defined as the number of sources around real radio positions $n_{\text{real}}(\vartheta)$, reduced by the number of sources around mock radio positions $n_{\text{mock}}(\vartheta)$ and divided by the number of “real” matches.

We estimated $n_{\text{real}}(\vartheta)$ by counting the number of *WISE* sources detected in all four bands within circular regions of radius ϑ between $0''$ and $60''$ centered on a sample of $5 \cdot 10^4$ sources randomly extracted from each of the three radio surveys. The value of $n_{\text{mock}}(\vartheta)$ was calculated by averaging over one hundred mock realizations of the coordinates of each real radio source, generated by moving the real position in a random direction and by a random radial distance in the $[60, 120]''$ range.

The maximum cross-match radii evaluated for the NVSS and SUMSS surveys are $\vartheta_{\text{NVSS}} = 10''.4$, $\vartheta_{\text{SUMSS}} = 7''.4$ respectively, identical to those determined for the 1st release of the WIBRaLS catalog. This approach does not work for the FIRST survey because of the very high density of FIRST sources. For this reason, we assume as optimal search radius for FIRST the value previously determined $\vartheta_{\text{FIRST}} = 3''.4$ (Paper I), that was obtained by combining conservative estimates of the positional uncertainties of FIRST and All *WISE* sources.

The number of *WISE* blazar-like sources associated with at least one radio counterpart in either of the three surveys within the maximum radial distances discussed above is 32630, split in 18903 with a NVSS counterpart, 1040 with a FIRST counterpart and 3323 with a SUMSS counterpart. In order to exclude *WISE* sources associated to distinct radio sources associated to the emission of lobes of the same radio galaxy, we searched and removed all duplicate radio sources whose positions would fall within $6'$ from each other. This radius matches the typical positional uncertainty of γ -ray sources detected by LAT in the 3FGL (Acero et al. 2015). In these cases, the All *WISE* source with the largest score among all the duplicates was retained. After this step, the number of *WISE* blazar-like sources with a radio counterpart in the NVSS, FIRST and SUMSS catalogs is 18693, 10227 and 3287 respectively, for a total of 32207 sources. This sample includes 5547 sources with a counterpart from both the NVSS and FIRST surveys and 709 sources with one counterpart from both NVSS and one SUMSS. The number of unique *WISE* blazar-like sources associated to a radio counterpart (i.e., the previous sample after removing sources with radio counterpart listed in

two catalogs) is 25951, with $\sim 72\%$ (18693) has a NVSS counterpart, $\sim 18\%$ (4687) has a FIRST counterpart and the remaining $\sim 10\%$ (2578) are associated to a FIRST source. Moreover, 7101 sources ($\sim 27\%$) of this list are classified as candidate BZBs, 2186 ($\sim 8\%$) as Mixed candidates and the remaining 1664 ($\sim 64\%$) as candidate BZQs², with 1366 class A ($\sim 5\%$), 3302 class B ($\sim 13\%$), 9265 class C ($\sim 36\%$) and the remaining 12018 ($\sim 47\%$) as class D sources.

3.3. Radio-loudness selection

Blazars are radio-loud AGNs but not every radio-loud AGN is a blazar. Blazars are generally hosted in elliptical galaxies, whose emission at radio frequencies is dominated by synchrotron emission from particles accelerated in the AGN relativistic jet pointed along the line of sight. In order to distinguish blazars from other radio sources, when lacking radio spectral information, we adopted the approach described in what follows. Padovani et al. (2011) as well as Bonzini et al. (2013) suggested that AGN-powered radio-sources can be identified using q_{24} , a modified definition of the so-called q parameter (Helou et al. 1985), i.e. the logarithm of the ratio of far-IR to radio flux density, to overcome the dearth of accurate flux density measurements at far-IR frequency. The q_{24} parameter is defined as:

$$q_{24} = \log(S_{24\mu m}/S_{1.4\text{GHz}}) \quad (1)$$

where $S_{24\mu m}$ is the observed flux density at $24\mu m$ and $S_{1.4\text{GHz}}$ is the flux density measured at 1.4 GHz. Following D’Abrusco et al. (2014), we adopted a similar criterion to select “radio-loud sources” among the *WISE* blazar-like sources with a radio-counterpart by using the parameter q_{22} defined as:

$$q_{22} = \log(S_{22\mu m}/S_{\text{radio}}) \quad (2)$$

where the flux density in the $24\mu m$ band of the Multi-band Imaging Photometer used on *Spitzer* (MIPS) is replaced by the *WISE* W4 ($[22]\mu m$) band. This approach is possible thanks to the similarities of the two wavebands (see Paper I for additional details). For the S_{radio} in Equation 2 we used the radio flux density at 1.4 GHz for sources with a NVSS or FIRST radio counterparts. Given the lack of flux measurement at 1.4 GHz for SUMSS sources, for those sources we used flux densities at 843 MHz.

Due to the remarkable flatness of radio spectra of blazars (see e.g., Healey et al. 2007; Massaro et al. 2013d), replacing the flux density at 1.4 GHz with the same quantity at 843 MHz produces a small effect of the value of the q_{22} parameter, whose size was estimated using the sample of *WISE* blazar-like sources with a radio counterpart detected in both NVSS and SUMSS (508 sources). The distribution of the difference between the values of $q_{22}(1.4\text{ GHz})$ and $q_{22}(843\text{ MHz})$ is fairly constant across the interval of $q_{22}(1.4\text{ GHz})$ covered by our sample, with $\Delta q_{22} \approx -0.07$, confirming a fairly flat radio spectrum for the sources in this sample. Based on this finding, for the *WISE* blazar-like sources associated with SUMSS counterparts only, we have used the corrected q_{22} value defined as $q'_{22}(843\text{ MHz}) = q_{22}(843\text{ MHz}) + \Delta q_{22}$.

Both the q_{24} and q_{22} parameters show a dependence on the redshift of the source, as their values decrease for larger redshifts (Bonzini et al. 2013; D’Abrusco et al. 2014). Figure 1 shows the distribution of q_{22} values for the confirmed γ -ray emitting blazars in the *locus* sample with reliable redshift measurements, as a function of the redshift and color-coded according to their spectral classification from the BZCat. *Locus* sources (mostly BZBs) with uncertain or unknown redshifts were not used, reducing the number of *locus* members to 563 (split in 159 BZBs and 404 BZQs). In Figure 1, the same trend reported by Bonzini et al. (2013) and Paper I is observed. If redshift estimates were available for all *WISE* blazar-like sources associated to a radio counterpart, we could have determined different q_{22} thresholds in different redshift bins. Since redshifts are not available, we used fixed values of q_{22} .

In this paper, we improve over the approach used in Paper I by determining different q_{22} thresholds for *WISE* blazar-like sources with radio counterpart classified as candidate BZQs, BZBs and Mixed. The thresholds for candidate BZBs and BZQs, calculated as the 95% of the q_{22} distribution of all blazars in the *locus* sample classified as BZB and BZQ, are $q_{22}^{\text{BZB}} \leq -0.61$ and $q_{22}^{\text{BZB}} \leq -0.97$, respectively. The threshold for Mixed sources is set to the mean value of the thresholds for candidate BZQs and BZBs, $q_{22}^{(\text{Mixed})} \leq -0.79$. These thresholds are shown as horizontal lines in Figure 1.

We evaluated the effect of the unknown underlying redshift distribution of the *WISE* blazar-like sources with radio counterpart on our selection based on fixed q_{22} thresholds. We followed the same strategy used in Paper I. We computed the q_{22} for all sources in the *locus* sample after varying their observed redshifts over an equally spaced grid covering

² The selection of candidate BZQs using solely their *WISE* photometry can be contaminated by normal quasars as they share the same region of the *WISE* colors space (Wright et al. 2010). Also, the existence of radio counterparts to *WISE*-selected BZQ candidates alone, lacking radio spectral characterization, does not remove the degeneracy (Stern et al. 2005, 2012)

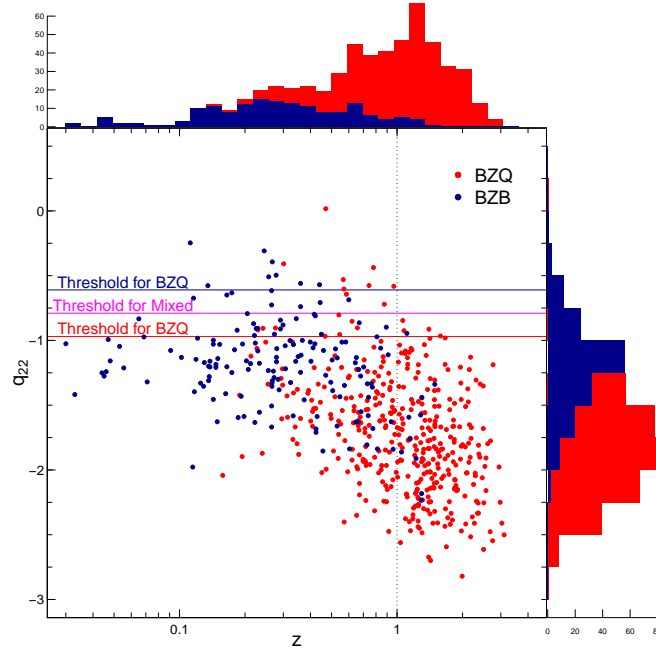


Figure 1. Scatterplot of the q_{22} values for the confirmed γ -ray emitting blazars in the *locus* sample as a function of their redshifts reported in the BZCat (Massaro et al. 2015). The red, magenta and blue horizontal lines show the values of the q_{22} thresholds used to select WIBRaLS sources among the *WISE* blazar-like sources with a radio counterparts for *WISE*-based classes of candidate BZQs, Mixed and BZBs (see Section 3.3).

Table 2. Members of the WIBRaLS catalog, split according to their *WISE* spectral types and classes, and provenance of the radio counterpart.

	BZB-like	Mixed	BZQ-like	Total
Class A	55	5	61	121
Class B	273	124	317	714
Class C	1086	579	1746	3411
Class D	2330	0	2965	5295
NVSS	3024	557	4093	7664
FIRST	36	7	21	64
SUMSS	694	144	975	1813
Total	3744	708	5089	9541

the $[0, 4]$ range with bins of 0.05 width, which includes the interval $[0, \sim 1.25]$ covered by the observed redshifts. We assumed power-law spectral energy distribution with slope constrained by the observed flux densities at $22 \mu\text{m}$ and at 1.4 GHz. The fractions of candidate BZQs and BZBs that satisfy the q_{22} conditions based on the observed redshift distribution are $\sim 91\%$ and $\sim 93\%$, respectively. These fractions are slightly lower than the $\sim 94\%$ fraction of sources recovered with the $q_{22} \leq -0.5$ threshold used in Paper I.

The total number of *WISE* blazar-like sources with a radio counterpart that satisfies the radio-loudness criteria based on the q_{22} parameter and, thus, belong to the second release of the WIBRaLS catalog is 9541. The break-down of the catalog according to *WISE* spectral type, class and provenance of the radio counterpart is given in Table 2,

Table 3. Sample of rows of the catalog of WIBRaLS sources.

All <i>WISE</i> name ^a	R.A. ^b	Dec. ^c	W1-W2 ^d	W2-W3 ^e	W3-W4 ^f	<i>s</i> _{BZB} ^g	<i>s</i> _{MIX} ^h	<i>s</i> _{BZQ} ⁱ	Class ^j	Type ^k	Radio counterpart ^l	<i>S</i> _{radio} ^m	<i>q</i> ₂₂ ⁿ
J000011.09-433316.4	0.0462203	-43.5545611	1.31	2.85	2.67	0.0	0.0	0.39	D	BZQ	SUMSSJ000011.2-433317	70.9	-1.41
J000020.40-322101.2	0.0850076	-32.3503443	1.35	3.26	2.47	0.0	0.0	0.52	C	BZQ	NVSSJ000020-322059	520.9	-1.94
J000029.07-163620.2	0.1211645	-16.6056221	0.39	2.01	2.45	0.53	0.0	0.0	C	BZB	NVSSJ000029-163621	89.1	-1.24
J000047.05+312028.2	0.1960452	31.3411703	0.82	2.48	2.4	0.32	0.0	0.0	D	BZB	NVSSJ000047+312027	46.4	-1.43
J000056.54-402206.4	0.235613	-40.368453	0.71	2.69	2.6	0.28	0.0	0.0	D	BZB	SUMSSJ000056.7-402208	76.0	-1.36
J000101.04+240842.5	0.2543718	24.1451458	1.23	3.06	2.13	0.0	0.0	0.34	D	BZQ	NVSSJ000101+240842	46.6	-1.26
J000105.29-155107.2	0.2720486	-15.8520035	1.18	3.42	2.14	0.0	0.0	0.33	D	BZQ	NVSSJ000105-155106	347.5	-2.01
J000108.11-373857.1	0.2838199	-37.6492076	1.32	2.72	2.29	0.0	0.0	0.39	D	BZQ	SUMSSJ000108.0-373901	23.1	-1.12
J000118.01-074626.9	0.3250683	-7.7741395	0.95	2.58	2.19	0.64	0.13	0.0	C	BZB	NVSSJ000118-074626	208.4	-1.23
J000131.63+165413.8	0.3818138	16.9038342	1.21	2.92	2.45	0.0	0.0	0.59	C	BZQ	NVSSJ000131+165416	63.1	-1.08
J000132.22+135258.4	0.3842501	13.8829081	1.07	3.0	2.48	0.0	0.0	0.23	D	BZQ	NVSSJ000132+135258	74.2	-1.59
J000132.34+240230.3	0.3847546	24.0417769	0.85	2.14	1.84	0.81	0.0	0.0	B	BZB	NVSSJ000132+240231	359.2	-1.28
J000132.74-415525.2	0.3864515	-41.9236926	0.68	2.17	2.09	0.48	0.0	0.0	D	BZB	SUMSSJ000133.1-415526	11.6	-0.84
J000132.83+145607.9	0.3868025	14.9355453	0.92	2.85	2.77	0.0	0.1	0.31	D	BZQ	NVSSJ000132+145609	314.6	-1.69
J000137.07+431543.9	0.4044828	43.2622002	0.72	2.61	2.32	0.76	0.0	0.0	B	BZB	NVSSJ000137+431544	61.8	-0.9

NOTE—(a): *WISE* name; (b): Right Ascension (J2000); (c): Declination (J2000); (d): W1-W2 *WISE* color; (e): W2-W3 *WISE* color; (f): W3-W4 *WISE* color; (g): Score for the BZB region of the *locus*; (h): Score for the Mixed region of the *locus*; (i): Score for the BZQ region of the *locus*; (j): Class (see Section 3.1); (k): Spectral type (see Section 3.1); (l): Name of the radio counterpart; (m): Radio flux density [mJy]; (n): Radio-loudness parameter *q*₂₂

while the basic parameters for a subset of sources in the catalog are displayed in Table 3. The number of sources of the *locus* sample of confirmed γ -ray emitting blazars used to determine the WIBRaLS selection, that are found in the final WIBRaLS2 is 666, $\sim 26\%$ less than the original size of the *locus* sample (901 sources). The exclusion of these 235 *locus* sources is the result of a) the definition of the *WISE* model (Section 3.1), that excludes 2% of the sources based on their location along the PC1 axis, and 5% of each spectral class because the radii of the three cylinders are defined to contain the 95% of associated sources, and b) the definition of the *q*₂₂ thresholds (Section 3.3), which remove 5% of the remaining *locus* sources for each spectral class, by definition.

4. CATALOG OF *WISE* γ -RAY BL LAC CANDIDATES

As mentioned briefly in Section 2.1, only $\approx 2.5\%$ of the All *WISE* sources are detected at $[22] \mu\text{m}$. For this reason, the WIBRaLS catalog, that requires its members to be detected in all four *WISE* bands, will certainly be incomplete for BZBs whose SEDs peak in the X-rays and are not bright enough to be detected in the W4 *WISE* band. This occurrence is schematically displayed in Figure 2, where the typical shapes of the SEDs of HBLs and LBLs are plotted together with the *WISE* sensitivity limits for the four *WISE* filters.

We designed a novel method that relies only on the colors obtained with the W1, W2 and W3 *WISE* bands to produce a list of candidate BL Lacs, extracted from the All *WISE* survey. The steps adopted for our procedure can be summarized as follows:

1. We select all All *WISE* sources detected only in the first three *WISE* bands, having IR colors similar to those of known *Fermi* BZBs belonging to the ROMA-BZCat v5.0.
2. From this sample, we further select only those sources with a radio counterpart in either one of the NVSS, SUMSS and FIRST radio surveys.
3. We identify as candidate BZBs sources whose values of the radio-to-infrared flux density ratio are compatible with those of confirmed *Fermi* BL Lacs.

Details on these steps are given in the following sections.

4.1. *WISE* color selection of BZB-like sources

The training set used to identify the *WISE* mid-IR colors of BL Lac objects was built selecting all the *Fermi* sources belonging to the 3FGL and associated with BZBs in the latest release of the Roma-BZCAT catalog (Massaro et al. 2015). We only considered sources whose All *WISE* counterparts are not detected in the W4 band. The total number of unique sources in the training set is 93. Among these sources, 34 are associated with a NVSS radio counterpart only, 3 are associated with a FIRST source only and the remaining 56 have both a NVSS and FIRST counterpart.

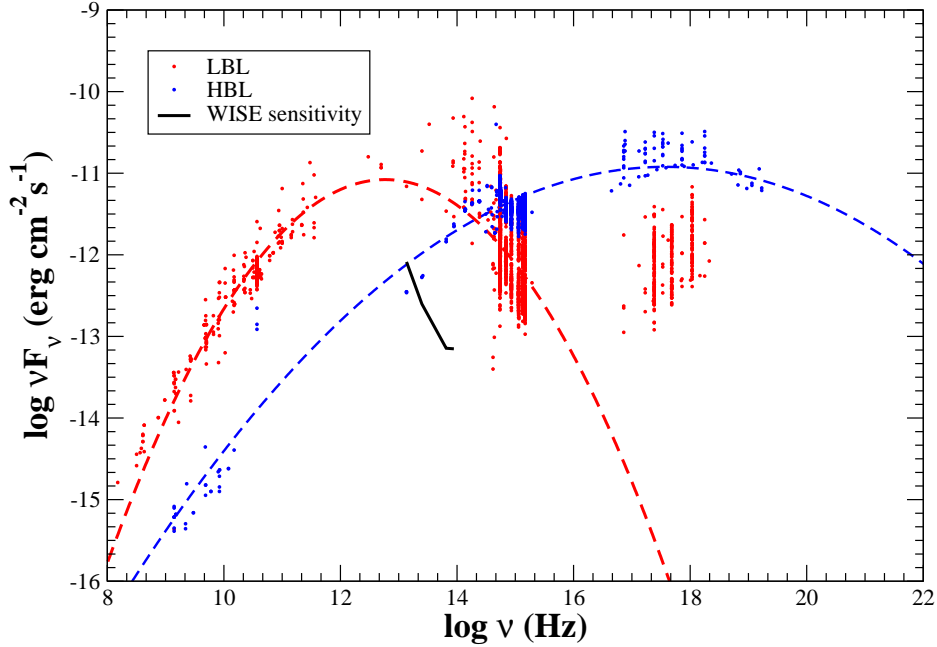


Figure 2. Historical SEDs of the two BZBs 1H 1426+428 (blue points), a TeV HBL, and AO 0235+164 (red points), a typical LBL (see Massaro et al. 2008a,b, respectively). Dashed lines represent the best fit log-parabolic functions used to describe their synchrotron components. The sensitivity limits in the *WISE* 4 bands are shown as a solid black line.

We selected *WISE* sources with IR colors similar to those of our training set by adopting the same procedure used in previous analyses (see e.g. Massaro et al. 2011; Paggi et al. 2013; Massaro et al. 2013a), based on the Kernel Density Estimation (KDE). KDE is a non-parametric procedure that estimates the Probability Density Function (PDF) of a multivariate distribution with no assumption on the properties of the parent population. The KDE depends on only one parameter, i.e., the bandwidth of the kernel of the density estimator, which is qualitatively analogous to the window size for one-dimensional running average.

We applied the KDE to the 2-dimensional distribution of training set sources in the *WISE* W2-W3 vs W1-W2 color-color plane to determine its PDF. Then, we selected infrared sources in the All *WISE* catalog not detected in the W4 passband and detected in the other three filters, whose colors are located within the isodensity contour enclosing 90% of the BL Lac training set. Only sources whose colors uncertainties ellipses are entirely contained within the 90% isodensity contour were retained. Figure 3 shows the distribution of the training set in the *WISE* color plane, together with the iso-density contours determined by the KDE method, with the 90% contour displayed as a thick black line. The projections on this color-color diagram of the W1BRLS2 catalog is also shown for reference.

The total number of *WISE* sources extracted applying this method is ~ 14406 , corresponding to $\sim 0.01\%$ of the parent sample of All *WISE* sources not detected only in W4.

4.2. Radio counterparts

We further select possible BL Lacs candidates by searching for radio counterparts of the sample of sources selected based on their *WISE* colors. This procedure obviously misses “radio weak BL Lacs” but to date they are extremely rare and their associations with *Fermi* sources has not yet been verified (Massaro et al. 2017; Bruni et al. 2018).

We crossmatched the color-selected *WISE* sources with the radio surveys NVSS, SUMSS and FIRST using the same maximum association radii established as described in Section 3.2. We found a total of 17826 sources with at least one radio counterpart: 5532 are associated with a FIRST source within $3''.4$, 10166 with a NVSS source within $10''$ and the remaining 2128 with a SUMSS source with $7''.4$ (see Table 4). After removing from our list sources with SUMSS

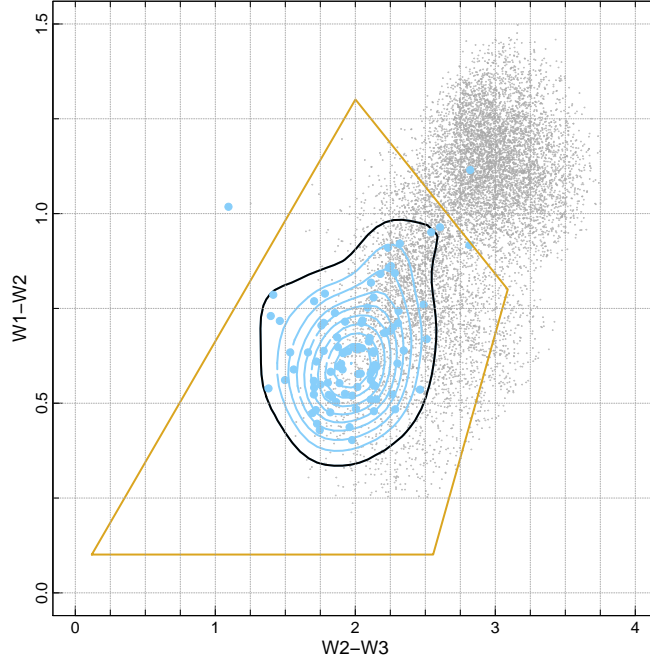


Figure 3. *WISE* W2-W3 vs W1-W2 color-color diagram. The 93 sources in the training set are shown by light blue circles, and the black line is the contour containing 90% of the sources in the training set and used to select the candidate KDE BL Lacs. Sources in the WIBRaLS catalog are displayed in the background for comparison (small gray circles). The yellow polygon shows the region in the *WISE* colors plane sources from the 2WHSP catalog are located (Chang et al. 2017) (see Section 5.1).

or FIRST counterparts that are also associated with a NVSS source, there remain 2099 *WISE* sources with a unique FIRST counterpart, 1680 *WISE* sources with a unique SUMSS counterpart and the 10166 associated with a NVSS radio source, for a total of 13945 sources. Similarly at what was done for the WIBRaLS catalog in Section 4.2, in order to avoid possible contamination from radio lobes originating from radio-galaxies, we also checked for sources that had from another radio source closer than $6'$, and, for FIRST radio counterparts only, sources with side lobe probability ≥ 0.05 . These constraints reduced the number of sources to 2049 sources with a unique FIRST counterpart, 1671 sources associated to a unique SUMSS source and 10084 with a radio counterpart in NVSS, for a total of 13804 candidates.

4.3. Infrared-to-radio ratio selection

The last step of the procedure to select *WISE* BL Lac candidates is based on the characterization of the distribution of their infrared-to-radio ratios q_{12} , similar to the q_{22} parameter used to select WIBRaLS sources 3.3. We define the parameter q_{12} as:

$$q_{12} = \log(S_{12\mu m}/S_{\text{radio}}) \quad (3)$$

i.e., the logarithm of the ratio between the *WISE* flux density measured in the W3 passband and the radio flux density. Flux density at 20 cm has been used to calculate q_{12} of sources with a unique counterpart in the NVSS and FIRST surveys. Given the flatness of the radio spectrum of BL Lacs (Healey et al. 2007; Massaro et al. 2013a) and our estimate of the $\Delta q_{22} \approx -0.07$ for the *WISE* -selected sources with both SUMSS and NVSS radio counterparts (see Section 3.3), we assume a flat spectrum ($\alpha_{\text{radio}} = 0$) and use the flux density at 36 cm to calculate the q_{12} parameter for sources with SUMSS counterparts.³

We consider BL Lac candidates those sources whose q_{12} values are consistent with the observed q_{12} distribution of the training set sources. The q_{12} values for sources with a FIRST or NVSS radio counterpart (59 and 90 respectively)

³ We estimate that for radio spectra with $\alpha_{\text{radio}} = \pm 0.1$, the effect on the values of $q_{12}(843 \text{ MHz})$ calculated at 36 cm for SUMSS counterparts would be a factor ranging from ≈ 0.95 to ≈ 1.05 . In the case of a much larger spectral index $\alpha_{\text{radio}} = 0.5$, the corrective factor would still be ≈ 0.77 .

have been used separately to determine the intervals of acceptable q_{12} values for both surveys, as in both surveys flux densities are measured at the same wavelength (20 cm).

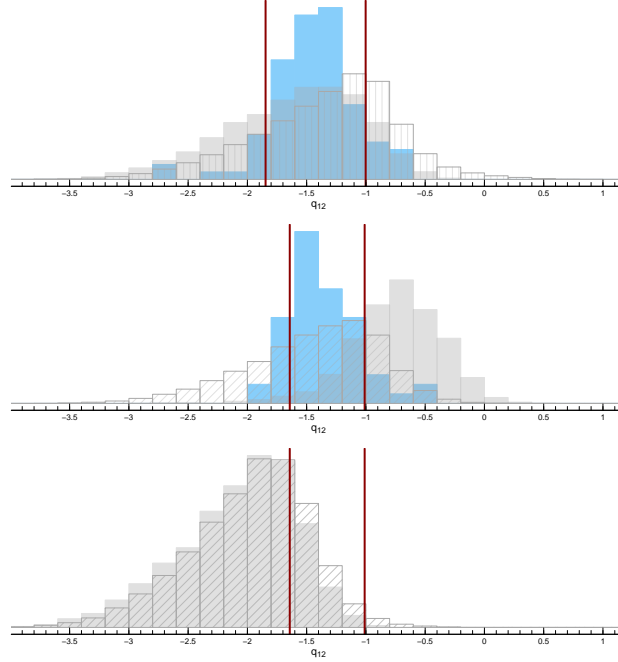


Figure 4. Upper panel: the light blue histogram shows the distributions of q_{12} values for confirmed γ -ray emitting BL Lacs (training set sources for the KDE candidate BL Lacs) with radio counterpart in the FIRST radio surveys. The solid and dashed gray histograms show the q_{12} distributions for a random sample of *WISE* sources associated with a FIRST counterpart and for the *WISE*-color selected candidate KDE BL Lacs, respectively. Mid panel: same as for upper panel for NVSS radio counterparts. Lower panel: q_{12} distributions for a random sample of *WISE* sources associated with a SUMSS radio source and for *WISE*-color selected candidate KDE BL Lacs (no training set sources with SUMSS radio counterparts are available). In all panels, vertical red lines display the 10-th and the 90-th percentiles of the q_{12} distribution of the training set used to select the final sample of sources in the KDEBLACS catalog (see Section 4.3).

Figure 4 shows the distributions of the q_{12} values of the BL Lacs training set sources (light blue histograms), control samples including random *WISE* sources with radio counterparts (solid gray histograms) and of the candidate BL Lacs selected according to their *WISE* colors as described in Section 4.1 (dashed gray histograms). FIRST (upper panel), NVSS (mid panel) and SUMSS (lower panel) radio counterparts are shown separately; the light blue histogram is missing from the SUMSS panel as no source in the training set has a radio counterpart from the SUMSS survey. It is also interesting to notice that the peaks of the distributions of q_{12} values for the control sample and the *WISE*-selected candidates with SUMSS radio associations (lower panel in Figure 4) are significantly shifted towards smaller values of q_{12} relative to the NVSS and FIRST distributions. This difference is due to relative shallowness of the SUMSS survey, whose sensitivity allows the detection of sources with minimum density flux at 36 cm $S_{\text{radio}}^{\text{SUMSS}}(36 \text{ cm}) = 5 \text{ mJy}$, larger than the $\sim 2 \text{ mJy}$ and $\sim 0.2 \text{ mJy}$ for NVSS and FIRST, respectively.

We defined the lower and upper limits of q_{12} values used to select the candidate BL Lacs as the 10-th and 90-th percentiles of the q_{12} distribution of the training set (red lines in Figure 4). The q_{12} intervals used to select the candidates are between -1.85 and -1 for NVSS training set sources and between -1.64 and -1.01 for sources with FIRST counterparts. Given the lack of training set BL Lacs with SUMSS counterpart, we have conservatively defined the upper and lower thresholds for the q_{12} selection of SUMSS BL Lac candidates as the highest and lowest values of the lower and upper thresholds on the q_{12} distribution of training set sources with a FIRST or NVSS counterpart, respectively. As a result, the interval of allowed q_{12} values for SUMSS counterparts ranges between -1.64 and -1. After applying the q_{12} selections to the sample of 13804 *WISE*-radio selected sources, we obtain 5941 candidates, split in 327 associated to a FIRST source, 5310 with a NVSS counterpart and the remaining 305 associated with a SUMSS source.

Table 4. Break-down of the number of *WISE* sources identified as BL Lacs candidate at each step of the selection described in Section 4, split by provenance of the radio counterparts.

	NVSS	FIRST	SUMSS	Total
<i>WISE</i> selection	10166	5532	2128	17826
duplicates removal	10166	2099	1680	13945
close sources removal	100084	2049	1671	13804
q_{12} selection	5310	327	305	5942
$\ b\ $ selection	4947	327	305	5579

Table 5. Sample of rows of the catalog of KDEBLACS.

All <i>WISE</i> name ^a	R.A. ^b	Dec. ^c	W1-W2 ^d	W2-W3 ^e	Radio name ^f	S _{20cm} ^g	q ₁₂ ⁱ
J000007.63+420725.5	0.0318093	42.1237527	0.35	1.92	NVSSJ000007+420722	18.2	-1.5
J000010.29-363405.2	0.042887	-36.5681267	0.53	2.33	NVSSJ000010-363407	6.2	-1.3
J000056.22-082742.0	0.2342813	-8.4616809	0.43	1.94	NVSSJ000056-082747	14.4	-1.6
J000116.37+293534.5	0.3182368	29.5929424	0.61	2.46	NVSSJ000116+293534	3.5	-1.02
J000126.44+733042.6	0.3601711	73.5118347	0.77	2.22	NVSSJ000126+733042	23.6	-1.63
J000137.86-103727.3	0.4077672	-10.6242584	0.40	2.07	NVSSJ000137-103727	10.2	-1.41
J000147.28+455015.2	0.4470018	45.8375759	0.78	1.91	NVSSJ000147+455016	4.2	-1.22
J000236.06-081532.4	0.6502775	-8.2590058	0.71	2.11	NVSSJ000236-081533	28.3	-1.61
J000302.99-105638.1	0.7624893	-10.9439389	0.67	2.36	NVSSJ000302-105637	18.2	-1.61
J000311.94-070144.3	0.7997588	-7.0289838	0.61	1.98	FIRST J000311.9-070144	4.17	-1.01

NOTE—(a): *WISE* name; (b): Right Ascension (J2000); (c): Declination (J2000); (d): W1-W2 *WISE* color; (e): W2-W3 *WISE* color; (f): Name of the radio counterpart; (g): Radio flux density [Jy]; (h): Radio-loudness parameter q_{12}

Then, as final step, we discarded all sources in the catalog located at Galactic latitudes $|b| < 10$ deg, since γ -ray sources at low galactic latitudes suffer from a higher detection threshold due to a higher Galactic diffuse emission background (Ackermann et al. 2015). This constraint reduces the total number of sources in the catalog of KDE-selected BL Lac candidates to 5579, due to the exclusion of 363 sources with a NVSS radio counterpart. In what follows, the sources in the catalog of KDE-selected candidate BL Lacs will be called KDEBLACS. The break-down of the number of BL Lacs candidates selected at different stages of the procedure as a function of the different radio surveys is displayed in Table 4, while the properties available for a sample of sources in the final KDEBLACS catalog is shown in Table 4

5. DISCUSSION

The full characterization of the two catalogs presented in this paper would require optical, spectroscopic follow-up observations to confirm the nature of the candidates, and will be discussed in a future paper. In this Section, we examine the global spatial and *WISE* photometric properties of the WIBRaLS2 and KDEBLACS catalogs, and discuss how they compare with the most recent catalogs of *Fermi* γ -ray sources.

The Aitoff projections of the sky positions in galactic coordinates of the WIBRaLS2 and KDEBLACS catalogs are shown in Figure 5. The coverage of the WIBRaLS2 catalog is mostly uniform across the sky (left panel in Figure 5), with the exception of a region along the galactic plane where radio sources are not available from any of the three surveys used. Two regions of higher density can be observed where the FIRST and SUMSS surveys overlap with the NVSS coverage, respectively north and south of the Galactic plane. In the right panel, the sky distribution of the KDEBLACS catalog features prominently a lower density of sources associated to SUMSS radio counterparts and the lack of sources due to the Galactic latitude selection described in Section 4.3.

It is interesting to compare the regions of the *WISE* color space occupied by the WIBRaLS2 and KDEBLACS catalogs. The location of the sources belonging to the above catalogs in the *WISE* color space is displayed in Figure 6. The two samples occupy partially overlapping but distinct regions of the three dimensional *WISE* color space. Since KDEBLACS are not detected in the W4 passband by definition, their positions along the W3-W4 axis cannot be

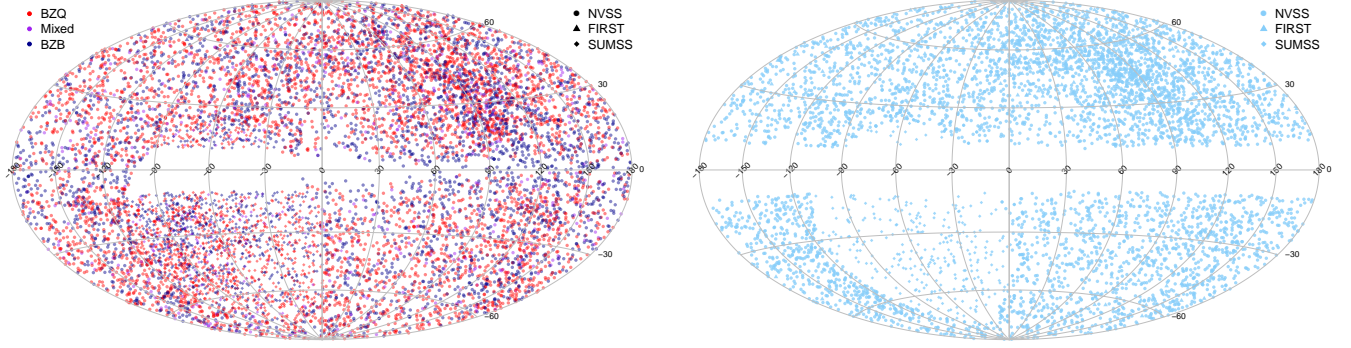


Figure 5. Left panel: Aitoff projection of the distribution in galactic coordinates of the WIBRaLS2 sources. The provenance of the radio counterpart and *WISE* spectral class of the candidate blazars are encoded in the shape and color of the symbols, respectively. Right panel: Aitoff projection of the distribution in galactic coordinates of the BL Lacs candidates selected with the KDE method. The provenance of the radio counterpart is encoded in the shape of the symbols.

established, but the three-dimensional volume of the space potentially occupied by these sources can be determined by using the upper limits on their W4 brightness (i.e., lower limits on their W4 magnitude) available in the All *WISE* catalog.

The two catalogs of blazar candidates described in this paper are complementary because their members can differ in spectral properties (see discussion in Section 4) and in brightness. Figure 7, that displays the histograms of the magnitude values for the three *WISE* filters W1, W2 and W3 for the WIBRaLS2 and KDEBLLACS samples together, confirms that the KDE-based method selects sources that are increasingly fainter than those in the WIBRaLS catalog as the wavelength increase going from filter W1 to W3.

5.1. Comparison with literature

One of the main goals of the production of catalogs of candidate blazars, like the two discussed in this paper, is the discovery of multi-wavelength counterparts of unassociated γ -ray sources (UGSs) observed by *Fermi*. While the thorough analysis that is necessary to reliably associate low energy candidate blazars to UGS (see, for example D’Abrusco et al. 2013; Massaro et al. 2015; Schinzel et al. 2015) is beyond the goals of this paper, as a consistency check and in order to assess the potential of the two catalogs here discussed to improve the characterization of the currently known γ -ray sources, we compared the WIBRaLS2 and KDEBLLACS catalogs with the most recent catalogs of sources detected by *Fermi* LAT.

We spatially crossmatched the WIBRaLS2 catalog with the 3FGL catalog (Acero et al. 2015) using the 98% elliptical uncertainty regions for 3FGL sources and a fixed positional uncertainty of $1''$ on the WIBRaLS2 radio coordinates. We found a total of 1049 matches, including the 666 sources in the *locus* sample selected as WIBRaLS2 members (see Section 3.3). Among the remaining 373 sources, 49 are unassociated; the 320 sources that are associated or identified with a known multi-wavelength counterpart in 3FGL are all classified, according to the CLASS1 parameter in 3FGL (Acero et al. 2015), as BL Lacs, FSRQs or BZU (Blazar candidate of Uncertain type), except for 3 rdg (radio-galaxies) and 3 ssrq (soft-spectrum radio quasars). The crossmatch between the KDEBLLACS catalog and 3FGL, using the same positional uncertainties, returned 186 matches (all distinct from the WIBRaLS2 crossmatches), with 57 unassociated sources. $\sim 95\%$ of the remaining 131 3FGL sources crossmatched with a KDEBLLACS source that are associated or identified, are classified as BZU or BL Lacs according to the 3FGL CLASS parameter. The total number of unique crossmatched sources from either the WIBRaLS2 or KDEBLLACS catalogs increases to 1757 (1404 and 353, respectively) when the preliminary LAT 8-year Point Source List (FL8Y)⁴ (which contains a total of 5523 γ -ray sources) is used, for a total of 152 unassociated sources. Out of the 1605 associated or identified sources, $\sim 99\%$ are classified as either BL Lacs, FSRQs or BZU.

Following the same approach described above, we also crossmatched the WIBRaLS2 and KDEBLLACS catalogs with the Third Catalog of Hard *Fermi*-LAT Sources (3FHL; Ajello et al. 2017a). The spatial crossmatch returns a total of 807 distinct matches, split in 647 from WIBRaLS2 and 160 from KDEBLLACS, with 33 unassociated 3FHL

⁴ <https://fermi.gsfc.nasa.gov/ssc/data/access/lat/fl8y/>

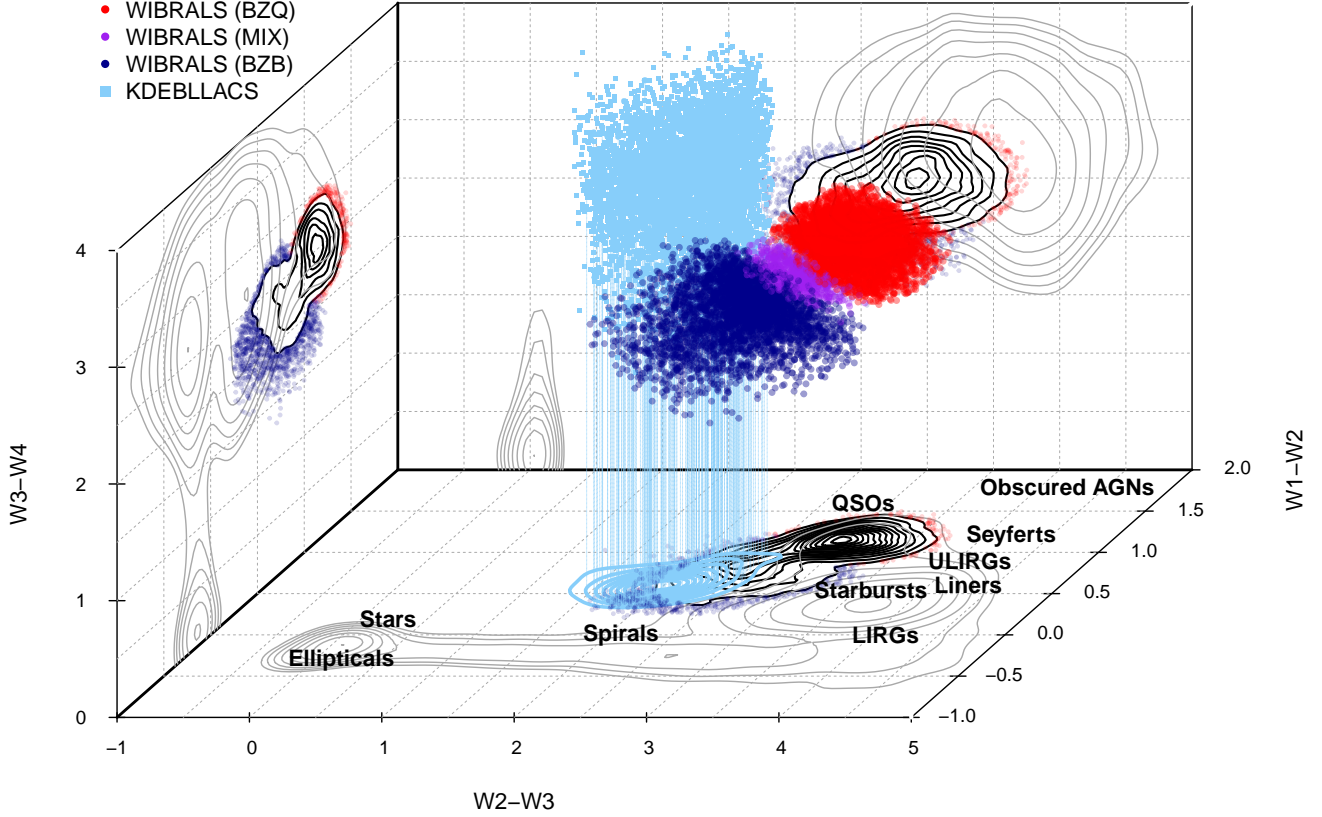


Figure 6. Distribution of the WIBRaLS2 and KDEBLACS (light blue) catalogs in the three-dimensional *WISE* color space. WIBRaLS2 sources are color-coded according to their *WISE* spectral classification, while the three-dimensional positions of the KDEBLACS sources (light blue), given their non-detection in the W4 filter, is visualized by using the lower limit in the W4 magnitude and by segments originating from these points and delimiting the 3-D volume in the color space where these sources may be actually located. The isodensity contours of the distributions of WIBRaLS2 (black) and KDEBLACS (blue light) samples are shown in the W2-W3 vs W1-W2 plane, while the gray lines on the three color-color planes represent the projected isodensity contours associated with 10 log-spaced levels of a sample of *WISE* random sources (including both sources detected and not detected at $22\ \mu\text{m}$). The approximate locations of different classes of sources in the W2-W3 vs W1-W2 color-color plane, according to [Wright et al. \(2010\)](#), are also shown for guidance.

sources and the remaining 774 composed by BL Lacs (520, $\sim 68\%$ of the total), and blazars of uncertain type (BZU, $\sim 16\%$ of the total). The 83% of the WIBRaLS2 members crossmatched with 3FHL sources are classified as candidate BZBs or MIXED candidates, based on their *WISE* colors.

It is also useful to compare the two catalogs of candidate blazars presented in this paper with the largest catalog of candidate HSPs available in the literature to date, namely the second WISE High Synchrotron Peaked blazar (2WHSP) catalog ([Chang et al. 2017](#)), with 1691 entries. The 2WHSP is an expansion of the 1WHSP catalog ([Arsioli et al. 2015](#)), and contains HSPs candidates drawn from the All*WISE* catalog that can be associated to radio and X-ray counterparts. The 2WHSPs candidates are further selected by requiring that their radio-to-IR and IR-to-X-ray broad-band spectral slopes are consistent with those of known, confirmed HSPs sources ([Chang et al. 2017](#)), and that the peak frequency of the synchrotron emission component of their SEDs ν_{peak} is $> 10^{15}$ Hz ([Chang et al. 2017](#)). The 2WHSP contains 1691 unique candidates or confirmed HSPs: 460 of these sources are associated to All*WISE* sources detected in four bands and 717 sources are associated to sources detected in the first three (W1, W2 and W3) filters.

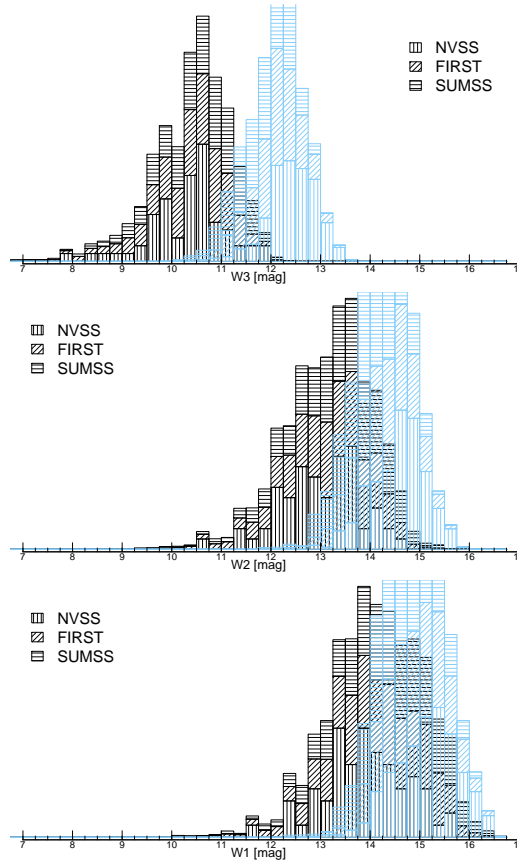


Figure 7. Distribution of magnitudes in the W1 (lower panel), W2 (mid panel) and W3 (upper panel) *WISE* filters for WIBRaLS2 (black histograms) and KDEBLACS (light blue histogram) candidate blazars, broken down by provenance of the radio counterpart.

The remaining sources cannot be compared to the catalogs discussed in this paper because not detected in both the W3 and W4 passbands. We determined that 248 of the 460 2WSHPs sources detected in all All *WISE* filters are also in the new WIBRaLS catalog, while 267 of the 717 sources not detected in W3 have been selected as KDEBLACS. The main cause of difference between our catalogs and the 2WSHP is the maximum spatial radius used to crossmatch All *WISE* sources with radio counterparts from one of the three radio surveys FIRST, NVSS and SUMSS. [Chang et al. \(2017\)](#) report that radio counterparts were selected within $0.3'$ and $0.1'$ for NVSS/SUMSS and FIRST catalogs, respectively. These radii are significantly larger than the radii used in this catalog, discussed in Sections 3.2 and 4.2 ($10''.4$, $3''.4$ and $7''.4$ for NVSS, FIRST and SUMSS respectively). As a consequence, only 311 All *WISE* sources with a unique radio counterpart contained in the sample used to extract the KDEBLACS can also be found in the 2WSHP catalog. Another possible source of difference between the KDEBLACS and the 2WSHP catalogs is the extent of the region in the *WISE* color-color diagram where 2WSHP sources are located, which is significantly larger than the area where the BL Lacs candidates are selected from (see Figure 3).

5.2. Comparison with the WIBRaLS1 catalog

The second release of the WIBRaLS catalog, WIBRaLS2, described in this paper, contains 5025 candidate blazars also found in the first WIBRaLS (WIBRaLS1 hereinafter) catalog (Paper I). Of the total 7885 members of WIBRaLS1, 2830 sources are not included in WIBRaLS2 because their q_{22} values (for $\sim 95\%$ of them) are larger than the new, more stringent thresholds adopted for BZQs in WIBRaLS2 (see Section 3.3). The increase in the size of the training set of confirmed γ -ray blazars used to define the WIBRaLS *locus* has led to an increase of the volume in *WISE* color space that has produced 4711 sources in the WIBRaLS2 not included in WIBRaLS1.

6. SUMMARY AND CONCLUSIONS

In this paper, we present two new catalogs of blazar candidates, selected on the basis of their *WISE* mid-IR colors, their association to a radio counterpart and their radio-loudness. These new catalogs contain a combined total of 15196 candidate blazars, including both candidate FSRQs and BL Lacs, distributed on $\sim 90\%$ of the sky.

The second, enhanced release of the WIBRaLS catalog supersedes the original WIBRaLS1 (Paper I) catalog, which has been extensively employed to associate *Fermi* unidentified sources with their low energy counterparts. WIBRaLS2 contains candidate blazars drawn from All *WISE* sources detected in all four *WISE* passbands with colors similar to those of spectroscopically confirmed, γ -ray emitting blazars, that are associated to radio counterparts and identified as radio-loud. Spectral classification as candidate BZBs, BZQs or Mixed candidate blazars, following the ROMA-BZCat (Massaro et al. 2015) terminology, and derived on the *WISE* color properties is also provided. WIBRaLS2 contains 9541 candidate blazars, a $\sim 25\%$ increase over the first version of WIBRaLS.

The KDEBLACS catalog complements the WIBRaLS2 by identifying BL Lacs candidates that, because of their typical low infrared-to-radio ratios and/or *WISE* brightness (cp. HBLs), have gone undetected in the W4 *WISE* filter and, as a consequence, cannot be considered for selection in WIBRaLS2. The KDEBLACS members are required to be detected in the three *WISE* filters W1, W2 and W3 and are selected based on their positions in the W2-W3 vs W1-W2 *WISE* color-color diagrams using the KDE technique. They are also associated to a radio counterpart and identified as radio-loud according to the q_{12} radio-to-MIR spectral parameter. We select 5579 sources in the KDEBLACS.

Previous samples of candidate blazars selected on the basis of the IR colors, eventually combined with radio and/or multifrequency observations (see e.g. Massaro et al. 2013e; Arsioli et al. 2015; Maselli et al. 2015; Massaro et al. 2016) have been used by the *Fermi*-LAT collaboration for the preparation of the 3FGL, the Third Catalog of Active Galactic Nuclei (3LAC; Ackermann et al. 2015) and the Second and the Third Catalog of Hard *Fermi*-LAT Sources (2FHL and 3FHL; Ackermann et al. 2016; Ajello et al. 2017a, respectively).

This work will contribute to a more comprehensive understanding of the diverse and fascinating γ -ray sky as observed by *Fermi*. In particular, the community will benefit from the WIBRaLS2 and KDEBLACS catalogs of candidate blazars presented in this paper and the subsequent programs of follow-up spectroscopic observations needed to confirm their nature and, possibly, determine their redshifts by using them to: (i) improve our knowledge of the luminosity function of BL Lacs (see e.g., Ajello et al. 2014); (ii) select potential targets for the Cherenkov Telescope Array (CTA) as shown by Massaro et al. (2013c); Arsioli et al. (2015); (iii) obtain more stringent limits on the dark matter annihilation in sub-halos (see e.g., Zechlin, & Horns 2012; Berlin et al. 2014); (iv) search for counterparts of new flaring γ -ray sources (see e.g., Bernieri et al. 2013) and of high energy neutrino emission (see e.g., IceCube Collaboration et al. 2018); (v) test new γ -ray detection algorithms (see e.g., Campana et al. 2015, 2016, 2017); (vi) and, finally, perform population studies of the remaining UGSs (see e.g., Acero et al. 2013).

REFERENCES

- Abdo, A. A., Ackermann, M., Agudo, I., et al. 2010, ApJ, 716, 30.
- Acero, F., Donato, D., Ojha, R., et al. 2013, ApJ, 779, 133.
- Acero, F., Ackermann, M., Ajello, M., et al. 2015, The Astrophysical Journal Supplement Series, 218, 23.
- Ackermann, M., Ajello, M., Atwood, W. B., et al. 2015, ApJ, 810, 14.
- Ackermann, M., Ajello, M., Atwood, W. B., et al. 2016, The Astrophysical Journal Supplement Series, 222, 5.
- Agudo, I., Thum, C., Gómez, J. L., et al. 2014, A&A, 566, A59.
- Ajello, M., Romani, R. W., Gasparrini, D., et al. 2014, ApJ, 780, 73.
- Ajello, M., Atwood, W. B., Baldini, L., et al. 2017, The Astrophysical Journal Supplement Series, 232, 18.
- Ajello, M., Atwood, W. B., Baldini, L., et al. 2017, The Astrophysical Journal Supplement Series, 232, 18.
- Álvarez Crespo, N., Massaro, F., D’Abrusco, R., et al. 2016, Ap&SS, 361, 316.
- Álvarez Crespo, N., Masetti, N., Ricci, F., et al. 2016, AJ, 151, 32.
- Álvarez Crespo, N., Massaro, F., Milisavljevic, D., et al. 2016, AJ, 151, 95.
- Angelakis, E., Hovatta, T., Blinov, D., et al. 2016, MNRAS, 463, 3365.
- Arsioli, B., Fraga, B., Giommi, P., et al. 2015, A&A, 579, A34.
- Becker, R. H., White, R. L., & Helfand, D. J. 1995, ApJ, 450, 559.
- Berlin, A., Hooper, D., & McDermott, S. D. 2014, PhRvD, 89, 115022.

- Bernieri, E., Campana, R., Massaro, E., et al. 2013, *A&A*, 551, L5.
- Best, P. N., Kauffmann, G., Heckman, T. M., et al. 2005, *MNRAS*, 362, 9.
- Blandford, R. D., & Rees, M. J. 1978, BL Lac Objects, 328.
- Bonzini, M., Padovani, P., Mainieri, V., et al. 2013, *MNRAS*, 436, 3759.
- Böttcher, M. 2007, *Ap&SS*, 309, 95.
- Böttcher, M. 2012, Relativistic Jets from Active Galactic Nuclei, 17.
- Bruni, G., Panessa, F., Ghisellini, G., et al. 2018, *ApJ*, 854, L23.
- Campana, R., Massaro, E., Bernieri, E., et al. 2015, *Ap&SS*, 360, 19.
- Campana, R., Massaro, E., & Bernieri, E. 2016, *Ap&SS*, 361, 185.
- Campana, R., Maselli, A., Bernieri, E., et al. 2017, *MNRAS*, 465, 2784.
- Chang, Y.-L., Arsioli, B., Giommi, P., et al. 2017, *A&A*, 598, A17.
- Chiaro, G., Salvetti, D., La Mura, G., et al. 2016, *MNRAS*, 462, 3180.
- Condon, J. J., Cotton, W. D., Greisen, E. W., et al. 1998, *AJ*, 115, 1693.
- Cowperthwaite, P. S., Massaro, F., D'Abrusco, R., et al. 2013, *AJ*, 146, 110.
- D'Abrusco, R., Massaro, F., Ajello, M., et al. 2012, *ApJ*, 748, 68.
- D'Abrusco, R., Massaro, F., Paggi, A., et al. 2013, *The Astrophysical Journal Supplement Series*, 206, 12.
- D'Abrusco, R., Massaro, F., Paggi, A., et al. 2014, *The Astrophysical Journal Supplement Series*, 215, 14.
- Dermer, C. D., & Schlickeiser, R. 1993, *ApJ*, 416, 458.
- Donoso, E., Best, P. N., & Kauffmann, G. 2009, *MNRAS*, 392, 617.
- Falomo, R., Pian, E., & Treves, A. 2014, *Astronomy and Astrophysics Review*, 22, 73.
- Giroletti, M., Massaro, F., D'Abrusco, R., et al. 2016, *A&A*, 588, A141.
- Gunn, J. E., Carr, M., Rockosi, C., et al. 1998, *AJ*, 116, 3040.
- Healey, S. E., Romani, R. W., Taylor, G. B., et al. 2007, *The Astrophysical Journal Supplement Series*, 171, 61.
- Helfand, D. J., White, R. L., & Becker, R. H. 2015, *ApJ*, 801, 26.
- Helou, G., Soifer, B. T., & Rowan-Robinson, M. 1985, *ApJ*, 298, L7.
- Homan, D. C., Ojha, R., Wardle, J. F. C., et al. 2002, *ApJ*, 568, 99.
- Hovatta, T., Lindfors, E., Blinov, D., et al. 2016, *A&A*, 596, A78.
- IceCube Collaboration, Aartsen, M. G., Ackermann, M., et al. 2018, *Science*, 361, eaat1378.
- La Mura, G., Chiaro, G., Ciroi, S., et al. 2015, *Journal of Astrophysics and Astronomy*, 36, 447.
- Landoni, M., Massaro, F., Paggi, A., et al. 2015, *AJ*, 149, 163.
- Landoni, M., Paiano, S., Falomo, R., et al. 2018, *ApJ*, 861, 130.
- Lister, M. L., & Homan, D. C. 2005, *AJ*, 130, 1389.
- Lister, M. L., Aller, H. D., Aller, M. F., et al. 2009, *AJ*, 137, 3718.
- Mainzer, A., Grav, T., Bauer, J., et al. 2011, *ApJ*, 743, 156.
- Marchesi, S., Kaur, A., & Ajello, M. 2018, *AJ*, 156, 212.
- Marchesini, E. J., Peña-Herazo, H. A., Álvarez Crespo, N., et al. 2019, *Ap&SS*, 364, 5.
- Maselli, A., Massaro, F., Cusumano, G., et al. 2013, *The Astrophysical Journal Supplement Series*, 206, 17.
- Maselli, A., Massaro, F., D'Abrusco, R., et al. 2015, *Ap&SS*, 357, 141.
- Massaro, F., Giommi, P., Tosti, G., et al. 2008, *A&A*, 489, 1047.
- Massaro, F., Tramacere, A., Cavaliere, A., et al. 2008, *A&A*, 478, 395.
- Massaro, E., Giommi, P., Leto, C., et al. 2009, *A&A*, 495, 691.
- Massaro, E., Giommi, P., Leto, C., et al. 2011, *Multifrequency Catalogue of Blazars (3rd Edition)*.
- Massaro, F., D'Abrusco, R., Ajello, M., et al. 2011, *ApJ*, 740, L48.
- Massaro, F., D'Abrusco, R., Tosti, G., et al. 2012, *ApJ*, 752, 61.
- Massaro, F., D'Abrusco, R., Tosti, G., et al. 2012, *ApJ*, 750, 138.
- Massaro, F., D'Abrusco, R., Paggi, A., et al. 2013, *The Astrophysical Journal Supplement Series*, 206, 13.
- Massaro, F., Giroletti, M., Paggi, A., et al. 2013, *The Astrophysical Journal Supplement Series*, 208, 15.
- Massaro, F., Paggi, A., Errando, M., et al. 2013, *The Astrophysical Journal Supplement Series*, 207, 16.
- Massaro, F., D'Abrusco, R., Giroletti, M., et al. 2013, *The Astrophysical Journal Supplement Series*, 207, 4.
- Massaro, F., D'Abrusco, R., Paggi, A., et al. 2013, *The Astrophysical Journal Supplement Series*, 209, 10.
- Massaro, F., Masetti, N., D'Abrusco, R., et al. 2014, *AJ*, 148, 66.
- Massaro, F., Landoni, M., D'Abrusco, R., et al. 2015, *A&A*, 575, A124.

- Massaro, E., Maselli, A., Leto, C., et al. 2015, *Ap&SS*, 357, 75.
- Massaro, F., D’Abrusco, R., Landoni, M., et al. 2015, *The Astrophysical Journal Supplement Series*, 217, 2.
- Massaro, F., Thompson, D. J., & Ferrara, E. C. 2015, *Astronomy and Astrophysics Review*, 24, 2.
- Massaro, F., Álvarez Crespo, N., D’Abrusco, R., et al. 2016, *Ap&SS*, 361, 337.
- Massaro, F. & D’Abrusco, R. 2016, *ApJ*, 827, 67.
- Massaro, F., Marchesini, E. J., D’Abrusco, R., et al. 2017, *ApJ*, 834, 113.
- Mauch, T., Murphy, T., Buttery, H. J., et al. 2003, *MNRAS*, 342, 1117.
- Mücke, A., & Protheroe, R. J. 2001, *Astroparticle Physics*, 15, 121.
- Murase, K., Dermer, C. D., Takami, H., et al. 2012, *ApJ*, 749, 63.
- Nolan, P. L., Abdo, A. A., Ackermann, M., et al. 2012, *The Astrophysical Journal Supplement Series*, 199, 31.
- Nori, M., Giroletti, M., Massaro, F., et al. 2014, *The Astrophysical Journal Supplement Series*, 212, 3.
- Orienti, M., D’Ammando, F., Giroletti, M., et al. 2014, *MNRAS*, 444, 3040.
- Padovani, P., & Giommi, P. 1996, *MNRAS*, 279, 526.
- Padovani, P., Miller, N., Kellermann, K. I., et al. 2011, *ApJ*, 740, 20.
- Paggi, A., Massaro, F., D’Abrusco, R., et al. 2013, *The Astrophysical Journal Supplement Series*, 209, 9.
- Paggi, A., Milisavljevic, D., Masetti, N., et al. 2014, *AJ*, 147, 112.
- Paiano, S., Falomo, R., Franceschini, A., et al. 2017, *ApJ*, 851, 135.
- Paiano, S., Landoni, M., Falomo, R., et al. 2017, *ApJ*, 844, 120.
- Paiano, S., Falomo, R., Treves, A., et al. 2019, *ApJ*, 871, 162.
- Pavlidou, V., Angelakis, E., Myserlis, I., et al. 2014, *MNRAS*, 442, 1693.
- Peña-Herazo, H. A., Marchesini, E. J., Álvarez Crespo, N., et al. 2017, *Ap&SS*, 362, 228.
- Ricci, F., Massaro, F., Landoni, M., et al. 2015, *AJ*, 149, 160.
- Schinzell, F. K., Petrov, L., Taylor, G. B., et al. 2015, *The Astrophysical Journal Supplement Series*, 217, 4.
- Stern, D., Eisenhardt, P., Gorjian, V., et al. 2005, *ApJ*, 631, 163.
- Stern, D., Assef, R. J., Benford, D. J., et al. 2012, *ApJ*, 753, 30.
- Stickel, M., Padovani, P., Urry, C. M., et al. 1991, *ApJ*, 374, 431.
- Taylor, M. B. 2005, *Astronomical Data Analysis Software and Systems XIV*, 29.
- Taylor, G. B., Healey, S. E., Helmboldt, J. F., et al. 2007, *ApJ*, 671, 1355.
- Takeuchi, Y., Kataoka, J., Maeda, K., et al. 2013, *The Astrophysical Journal Supplement Series*, 208, 25.
- Urry, C. M., & Padovani, P. 1995, *Publications of the Astronomical Society of the Pacific*, 107, 803.
- Vermeulen, R. C., & Cohen, M. H. 1994, *ApJ*, 430, 467.
- White, R. L., Becker, R. H., Helfand, D. J., et al. 1997, *ApJ*, 475, 479.
- Wright, E. L., Eisenhardt, P. R. M., Mainzer, A. K., et al. 2010, *AJ*, 140, 1868.
- Zechlin, H.-S., & Horns, D. 2012, *Journal of Cosmology and Astro-Particle Physics*, 2012, 50.

R.D'A. is supported by NASA contract NAS8-03060 (Chandra X-ray Center).

The work of F.M. and A.P. is partially supported by the “Departments of Excellence 2018-2022” Grant awarded by the Italian Ministry of Education, University and Research (MIUR) (L. 232/2016) and made use of resources provided by the Compagnia di San Paolo for the grant awarded on the BLENV project (S1618.L1.MASF.01) and by the Ministry of Education, Universities and Research for the grant MASF_FFABR.17.01. F.M. also acknowledges financial contribution from the agreement ASI-INAF n.2017-14-H.0 while A.P. the financial support from the Consorzio Interuniversitario per la fisica Spaziale (CIS) under the agreement related to the grant MASF_CONTR_FIN.18.02.

F.R. acknowledges support from FONDECYT Postdoctorado 3180506 and CONICYT project Basal AFB-170002.

V.C. is partially supported by the CONACyT research grant 280789

This research has made use of data obtained from the high-energy Astrophysics Science Archive Research Center (HEASARC) provided by NASA's Goddard Space Flight Center. The SIMBAD database operated at CDS, Strasbourg, France; the NASA/IPAC Extragalactic Database (NED) operated by the Jet Propulsion Laboratory, California Institute of Technology, under contract with the National Aeronautics and Space Administration. Part of this work is based on the NVSS (NRAO VLA Sky Survey): The National Radio Astronomy Observatory is operated by Associated Universities, Inc., under contract with the National Science Foundation and on the VLA low-frequency Sky Survey (VLSS). The Molonglo Observatory site manager, Duncan Campbell-Wilson, and the staff, Jeff Webb, Michael White and John Barry, are responsible for the smooth operation of Molonglo Observatory Synthesis Telescope (MOST) and the day-to-day observing programme of SUMSS. The SUMSS survey is dedicated to Michael Large whose expertise and vision made the project possible. The MOST is operated by the School of Physics with the support of the Australian Research Council and the Science Foundation for Physics within the University of Sydney. This publication makes use of data products from the Wide-field Infrared Survey Explorer, which is a joint project of the University of California, Los Angeles, and the Jet Propulsion Laboratory/California Institute of Technology, funded by the National Aeronautics and Space Administration. This publication makes use of data products from the Two Micron All Sky Survey, which is a joint project of the University of Massachusetts and the Infrared Processing and Analysis Center/California Institute of Technology, funded by the National Aeronautics and Space Administration and the National Science Foundation. TOPCAT⁵ (Taylor 2005) for the preparation and manipulation of the tabular data and the images.

⁵ <http://www.star.bris.ac.uk/~mbt/topcat/>